Original Article

Access this article online

Quick Response Code:

Website: http://www.braincirculation.org

DOI: 10.4103/bc.bc_40_23

Identification of brain endothelial cell-specific genes and pathways in ischemic stroke by integrated bioinformatical analysis

Yi Yan[1], Zhaohui Wang[1], Xiao Liu[1], Song Han[1,2], Junfa Li[1,2], Ying Zhang[1,2,3], Li Zhao[1,2]

[1]Department of Neurobiology, Capital Medical University, [2]Beijing Institute for Brain Disorders, Capital Medical University, [3]Beijing Key Laboratory of Hypoxia Conditioning Translational Medicine, Beijing, China

Address for correspondence:
Dr. Ying Zhang, Department of Neurobiology, Capital Medical University, Beijing 100069, China. Beijing Institute for Brain Disorders, Capital Medical University, Beijing 100069, China. Beijing Key Laboratory of Hypoxia Conditioning Translational Medicine, Beijing 100053, China.
E-mail: yingzhang@ccmu.edu.cn
Dr. Li Zhao, Department of Neurobiology, Capital Medical University, Beijing 100069, China. Beijing Institute for Brain Disorders, Capital Medical University, Beijing 100069, China.
E-mail: zhaoli@ccmu.edu.cn

Submission: 15-05-2023
Revised: 30-08-2023
Accepted: 08-09-2023
Published: 30-11-2023

Abstract:

BACKGROUND: Ischemic stroke (IS) is a life-threatening condition with limited treatment options; thus, finding the potential key genes for novel therapeutic targets is urgently needed. This study aimed to explore novel candidate genes and pathways of brain microvessel endothelial cells (ECs) in IS by bioinformatics analysis.

MATERIALS AND METHODS: The gene expression profiles of brain tissues or brain ECs in IS mice were downloaded from the online gene expression omnibus (GEO) to obtain the differentially expressed genes (DEGs) by R software. Functional enrichment analyses were used to cluster the functions and signaling pathways of the DEGs, while DEG-associated protein–protein interaction network was performed to identify hub genes. The target microRNAs and competitive endogenous RNA networks of key hub genes were constructed by Cytoscape.

RESULTS: Totally 84 DEGs were obtained from 6 brain tissue samples and 4 brain vascular EC samples both from IS mice in the datasets GSE74052 and GSE137482, with significant enrichment in immune responses, such as immune system processes and T-cell activation. Eight hub genes filtered by Cytoscape were validated by two other GEO datasets, wherein key genes of interest were verified by reverse transcription-polymerase chain reaction using an *in vitro* ischemic model of EC cultures. Our data indicated that AURKA and CENPF might be potential therapeutic target genes for IS, and Malat1/Snhg12/Xist-miR-297b-3p-CENPF, as well as Mir17 hg-miR-34b-3p-CENPF, might be RNA regulatory pathways to control IS progression.

CONCLUSIONS: Our work identified two brain EC-specific expressed genes in IS, namely, AURKA and CENPF, as potential gene targets for IS treatment. In addition, we presented miR-297b-3p/miR-34b-3p-CENPF as the potential RNA regulatory axes to prevent pathogenesis of IS.

Keywords:

Bioinformatics analysis, endothelial cells, gene expression omnibus datasets, ischemic stroke, RNA regulatory pathways

Introduction

Stemmed from brain arterial occlusion, ischemic stroke (IS) is the most common type of stroke and one of the leading causes of morbidity and mortality worldwide.[1,2] The only approved therapy for IS is to achieve rapid recanalization pharmacologically or surgically, which are both time-sensitive; thus, its application for most stroke patients is severely restricted yet.[3-6] Developing new therapeutic strategies is still a thorny task based on the divergent and complicated nature of stroke pathology.[7]

Notably, cerebral microvessel endothelial cells (ECs) constitute one of the essential components of blood–brain barrier (BBB).

How to cite this article: Yan Y, Wang Z, Liu X, Han S, Li J, Zhang Y, *et al*. Identification of brain endothelial cell-specific genes and pathways in ischemic stroke by integrated bioinformatical analysis. Brain Circ 2023;9:228-39.

Damage to brain ECs plays a key role in the pathophysiological progression of IS. Under ischemic condition, ECs are activated to lose tight junctions and then the corruption of BBB makes chance for immune cells to enter the brain parenchyma, leading to interstitial inflammation and vasogenic edema, which further exacerbates initial ischemia-caused neuronal damage and subsequent neurological deficit.[8-10] Restoring BBB and vasculature function, consequently alleviating neuroinflammation, now represents as a new mechanism to target.[11,12] Therefore, it is of great importance to investigate brain EC-specific target genes to expand the range of treatments available for IS.

As a gene detection technique over 10 years, gene chip or gene profile can be used to quickly detect the time-point expression information of all genes in a same sample, which is especially suitable for differential expression gene screening.[13,14] Currently, a large amount of sliced data are already generated and stored in public databases. Due to the target prediction using bioinformatics analysis, several biomarkers of endothelial dysfunction have been reported, such as miR-5-5p, ATF1, HSPA1, and DUSP.[15,16] Furthermore, therapeutic targets for IS such as hsa-miR-518-5p/hsa-miR-3135b have been reported.[17] However, in independent studies, the results were generated with very limited sample size, so their conclusions were with less accuracy of prediction. To address the shortcomings, an integrated bioinformatics approach by integrating and reanalyzing the data, combined with expression profiling techniques, would be an innovation to investigate reliable candidate genes and pathways which are closely associated with disease progressions.[18-20]

In this study, we first downloaded two gene expression omnibus (GEO) datasets of IS mice-derived brain tissues or brain ECs. After preprocessing and normalizating the data in R language, overlapped differentially expressed genes (DEGs) were identified between ischemic brain tissues and ECs. Next, the DEG's functional enrichment analyses, protein–protein interaction (PPI) network, as well as cluster modules and hub genes were analyzed and recognized. After validating the hub genes by another two GEO datasets, plus reverse transcription-polymerase chain reaction (RT-PCR) laboratory experiments, we finally identified two hub genes as EC-specific key genes of IS. The target microRNAs (miRNAs) and their coexpressed network of the two key genes were predicted by NetworkAnalyst and Cytoscape. In addition, competitive endogenous RNA (ceRNA) network was constructed according to the predictions of long noncoding RNAs (ncRNAs) and circular RNAs. Our study provided insight into the pathogenesis of IS at the transcriptome level and explored potential genes and RNA pathways as therapeutic options for IS.

Materials and Methods

Data retrieval

The GEO database was used in this study to acquire gene expression profiling data. We sought datasets of brain tissue or brain ECs in IS mice with the screening criteria as the following: (1) brain tissue or primary brain microvessels or ECs from adult C57BL/6 mice; (2) datasets contain middle cerebral artery occlusion (MCAO) group and control; (3) datasets contain at least three samples; and (4) datasets contain complete sample information. First, two RNAseq datasets GSE74052 and GSE137482 were chosen as test sets. GSE74052 contained 4 primary brain EC samples from transient MCAO-induced IS mice (1 h MCAO/R 1 day) and 4 control counterpart cell samples. GSE137482 contained 6 brain tissue samples from permanent distal MCAO mice and 6 control brain tissue samples, which were collected 3 days after stroke. Second, another two RNAseq datasets GSE167352 and GSE131193, both derived from mice with transient MCAO, were used as the validation sets. GSE163752 contained 5 brain ischemic EC samples (1 h MCAO/R 23 h) with 5 control cell samples. GSE131193 contained 3 ischemic brain microvessel samples from IS mice (1 h MCAO/R 1 or 7 days) and 3 control counterpart tissue samples [Table 1].

Data normalization and differentially expressed gene identification

The Limma software package (R4.1.3) Bioconductor, US was used to normalize the gene profiling data and to analyze the DEGs. The DEGs were filtered with adjusted $P < 0.05$, combined with fold change (FC) for upregulated (log2 [FC] >1) or downregulated (log2 [FC] <−1) genes, respectively. To better visualize the DEGs, the online tool Biofomatics was used to draw heatmaps, volcano plots and Venn diagram.

Table 1: Gene expression omnibus dataset information

GEO accession	Platform	Source	Samples		Attribute
			Control	IS	
GSE74052	GPL17021	Brain endothelial cells	4	4	Test
GSE137482	GPL19057	Brain tissues	6	6	Test
GSE163752	GLP19057	Brain endothelial cells	5	5	Validation
GSE131193	GPL19057	Brain microvessels	3	3	Validation

IS: Ischemic stroke, GEO: Gene expression omnibus

Protein–protein interaction network construction

The STRING database was used in this study to conduct PPI network of the DEGs, and the interaction relationship was visualized with Cytoscape software (v3.9.1) NIGMS, US. Minimal Common Oncology Data Elements (MCODE, version 2.0.0 University of Toronto, Toronto, Ontario, Canada) was used to identify highly interconnected gene clusters.[18] Significant genes in the network by using CytoHubba were considered as hub genes. Five algorithms in CytoHubba including Degree, Maximum Neighborhood Component (MNC), Density of MNC, Maximal Clique Centrality, Clustering Coefficient, were utilized to count the top 15 hub genes.[21,22] Lastly, the top genes were intersected to identify the final hub genes.

Functional enrichment analysis

DAVID (2021 Update, https://david.ncifcrf.gov/) was used to analyze the functional enrichment of the DEGs or the hub genes. The functional categories included Gene Ontology (GO) terms, Kyoto Encyclopedia of Genes and Genomes (KEGG) pathways, and reactome enrichment, with the cutoff criteria $P < 0.05$. GO enrichment results were figured as a horizontal bar plot using the PRISM 7 software (GraphPad), or a chord plot using GO plot software package (R4.1.3). The signaling pathway results were visualized as bubble charts using the online tool Biofomatics, or network by ClueGO (version 2.5.9) and CluePedia plugin (version 1.5.9) in Cytoscape (version 3.9.1) Laboratory of Integrative Cancer Immunology, France.

Receiver operating characteristic curve

The survival ROC package (R4.1.3) was used to plot ROC curves. The area under ROC curve (AUC) was calculated to quantify ROC. Sensitivity and specificity were calculated for optimum cutoff values.

Oxygen-glucose deprivation procedure

Culture of mouse brain microvascular ECs (bEnd. 3 cells) was performed as previous reports.[23] To mimic *in vitro* ischemia, bEnd. 3 cells were subjected to oxygen-glucose deprivation (OGD) medium (DMEM, no glucose) and placed in a closed hypoxia incubator (94% N_2, 5% CO_2, 1% O_2, 37°C). After 1 h of OGD treatment, cells were returned to normal medium in a normoxic incubator (95% air, 5% CO_2, 37°C) for 24 or 48 h.

Real-time quantitative reverse transcription-polymerase chain reaction

As we previously reported,[24] total RNA extraction and RT to produce cDNA were performed, and then the mRNA expressions of the interested genes were measured by SYBR Green qPCR SuperMix (4367659, Thermo, USA). The mRNA level of each gene was normalized with YWHAZ. The primers for YWHAZ were 5′-AGAGTCGTACAAAGACAGCAC-3′ and 5′-GAATGAGGCAGACAAAGGTTG-3′, the primers for AURKA were 5′-CTGGATGCTGCAAACGGATAG-3′ and 5′-CGAAGGGAACAGTGGTCTTAACA-3′, and the primers for CENPF were 5′-GCACAGCACAGTATGACCAGG-3′ and 5′-CTCTGCGTTCTGTCGGTGAC-3′.

Target microRNA prediction

The online miRNA database NetworkAnalyst and our previous dataset of 118 significantly expressed miRNAs in IS mouse brains[25] was employed to project miRNAs targeting the hub genes.

Competitive endogenous RNA network construction

StarBase (v 2.0) Chinese Academy of Sciences, China was used to explore lncRNAs (flter criteria: CLIP-data ≥1 and degradome-data ≥0) and circRNAs (flter criteria: CLIP-data ≥1 and degradome-data ≥2) which acted each other with the chosen miRNAs.[26] Depending on the interactions among mRNAs, miRNAs, and ncRNAs, a ceRNA network was created by Cytoscape.

Statistics analysis

The R software Limma package (R 4.1.3) Bioconductor, US was utilized to perform statistical analyses. Student's *t*-test was used when comparing the differences between two groups. GraphPad Prism 7.0 was used to analyze data and draw bar plots.

Results

Differentially expressed gene identification and analysis

The GSE74052 and GSE137482 datasets which included 4 brain tissues or 6 ECs both from IS mice were selected to analyze the DEGs. We obtained 2497 DEGs (1113 upregulated genes and 1384 downregulated genes) in GSE74052 and 1980 DEGs (1836 upregulated genes and 144 downregulated genes) in GSE137482 compared with genes in control samples [Figure 1a and b]. Volcano plots were used to better visualize the DEGs [Figure 1c and d]. Moreover, a total of 84 coincidentally upregulated (80 genes) or downregulated DEGs (4 genes) between GSE74052 and GSE137482 were identified by Venn analysis [Figure 1e].

Enrichment analysis

The 84 DEGs were categorized into three GO groups. Data showed that the DEGs were significantly enriched in immune system process, positive regulation of tumor necrosis factor production, activation of T cell and neutrophil, and other biological processes [Figure 2a]. The DEGs were significantly enriched in cellular components such as external side of plasma membrane

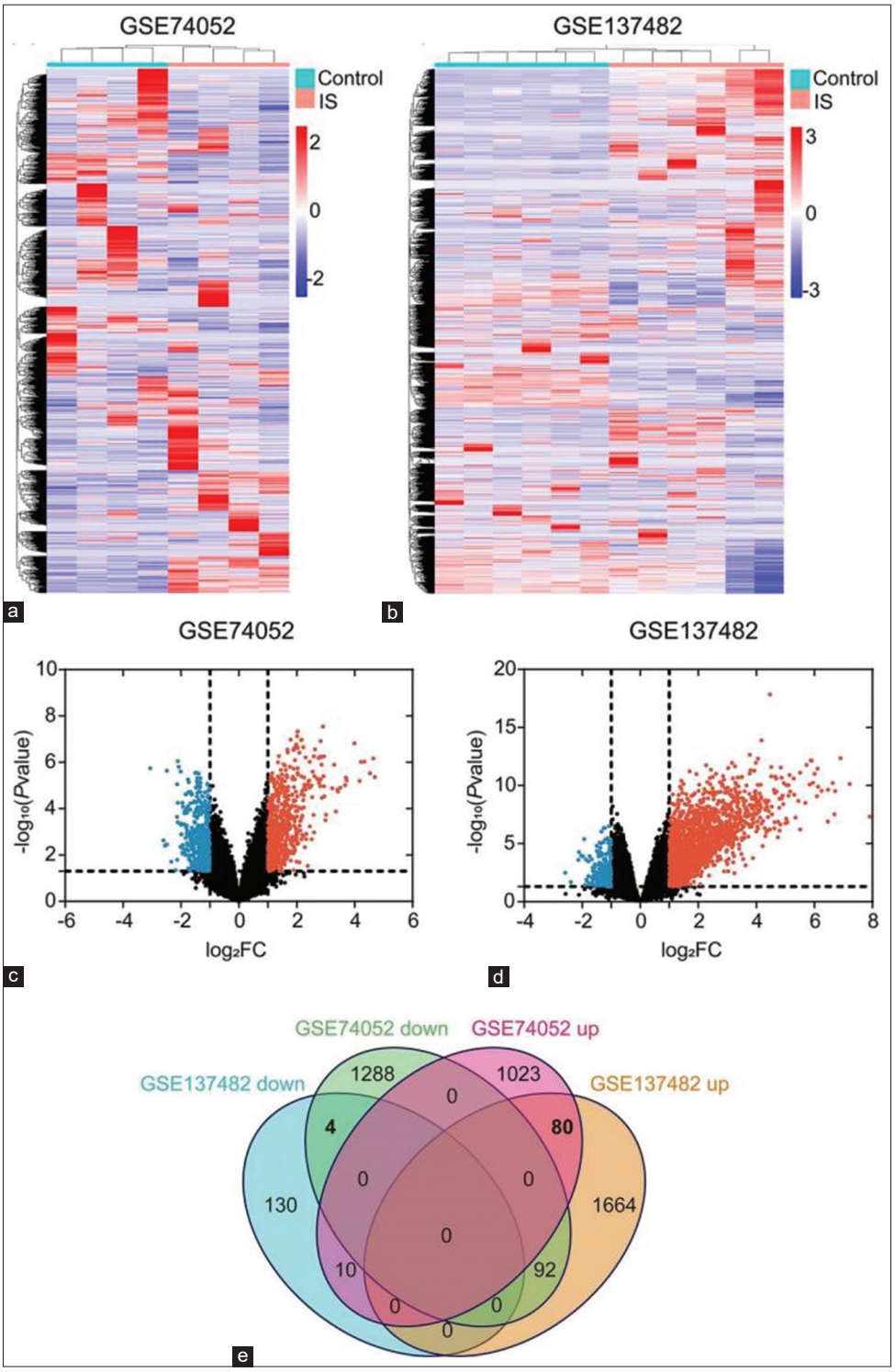

Figure 1: Identification of the differentially expressed genes (DEGs). (a and b) Heatmaps of the DEGs between ischemic stroke samples versus control ones in GSE74052 and GSE137482. Red rectangles represent high expression, and green rectangles represent low expression. (c and d) Volcano plots of DEGs ($|\log_2 FC| > 1$ and $P < 0.05$) from GSE74052 and GSE137482. Red plots represent upregulated genes, blue plots represent downregulated genes, and black plots represent nonsignificant ones. (e) Venn diagram showing the distribution of the DEGs in two datasets GSE74052 and GSE137482. IS: Ischemic stroke, FC: Fold change

and extracellular space [Figure 2a]. The DEGs were significantly enriched in molecular function such as identical protein binding and IgG binding [Figure 2a]. By KEGG pathway enrichment analysis, the DEGs were found mainly related with tuberculosis, protein digestion and absorption, NOD-like receptor signaling pathway, lipid and atherosclerosis, *staphylococcus aureus* infection, and thyroid hormone synthesis. Moreover, reactome pathway enrichment analysis indicated that the DEGs were significantly associated with pathways

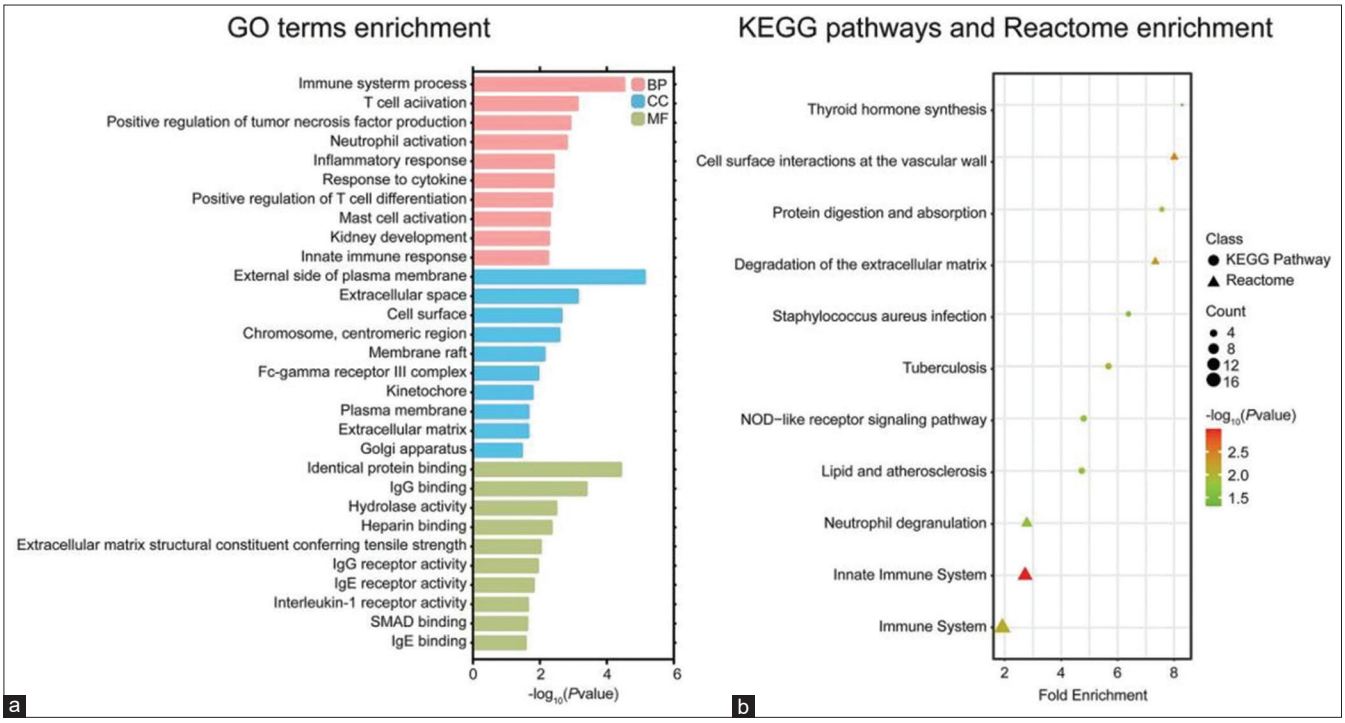

Figure 2: Functional enrichment analysis of the differentially expressed genes (DEGs). (a) Bar graph of representative enriched functional terms of three Gene Ontology groups: Biological process, cellular component, and molecular function. (b) The bubble plot showed the most enriched Kyoto Encyclopedia of Genes and Genomes (KEGG) and reactome pathways of the DEGs. Triangles, reactome enrichment terms; Circles, KEGG pathway terms. The X-axis depicts fold enrichment. The Y-axis lists the enriched functional terms or pathways. The larger the count value, the larger the shape size. GO: Gene ontology, KEGG: Kyoto encyclopedia of genes and genomes

such as innate immune system, cell surface interactions at the vascular wall, and degradation of the extracellular matrix [Figure 2b].

Protein–protein interaction network, minimal common oncology data elements cluster modules, and hub gene identification

These 84 DEGs built a PPI network with 48 nodes and 109 edges via STRING, which was illustrated by Cytoscape [Figure 3a]. As shown in Figure 3b-d, three modules were identified in the PPI network by MCODE plugin; Cluster 1 (score: 8, 8 nodes, 28 edges) scored the highest, followed by cluster 2 (score: 6.25, 9 nodes, 25 edges) and cluster 3 (score: 4.5, 5 nodes, 9 edges). Next, using five algorithms of cytoHubba plugin, 8 hub genes were finally identified: AURKA, OIP5, CENPF, CD84, EXO1, KNSTRN, MCM3, and RAD51 [Table 2].

Table 2: Cytohubba-identified 8 hub genes

Genes	Description	Regulation
AURKA	Aurora Kinase A	Up
OIP5	Opa Interacting Protein 5	Up
CENPF	Centromere Protein F	Up
CD84	CD84 Molecule	Up
EXO1	Exonuclease 1	Up
KNSTRN	Kinetochore Localized Astrin (SPAG5) Binding Protein	Up
MCM3	Minichromosome Maintenance Complex Component 3	Up
RAD51	RAD51 Recombinase	Up

Enrichment analysis of 8 hub genes

As shown in Figure 4a, the top enriched GO terms of the 8 hub genes were chromosome segregation (P = 4.87E–04), chromosome (P = 5.64E–04), spindle pole (P = 7.12E–04), microtubule organizing center (P = 9.95E–04), chromosome, centromeric region (P = 0.001), cell cycle (P = 0.001), perinuclear region of cytoplasm (P = 0.001), meiotic cell cycle (P = 0.002), nucleus (P = 0.004), and pronucleus (P = 0.005). KEGG pathways and reactome enrichment analyses indicated that the hub genes were mostly enriched in cell cycle [Figure 4b].

Receiver operating characteristic curves of the 8 hub genes in endothelial cells with ischemic insult

The GSE163752 (including 5 ischemic brain EC samples from IS mice) was used to analyze the expression profiles of 8 hub genes and draw the ROC curves. AUC is an evaluation index of the combination of sensitivity and specificity, thereby indicating the intrinsic effectiveness of interested genes.[27] The results determined all the 8 hub genes to have high AUC value (AUC >0.5), agreeing their close correlation to brain EC injury in IS. Among them, MCM3 (AUC: 0.933) showed the highest value, followed by EXO1 (AUC: 0.750), OIP5 (AUC: 0.733),

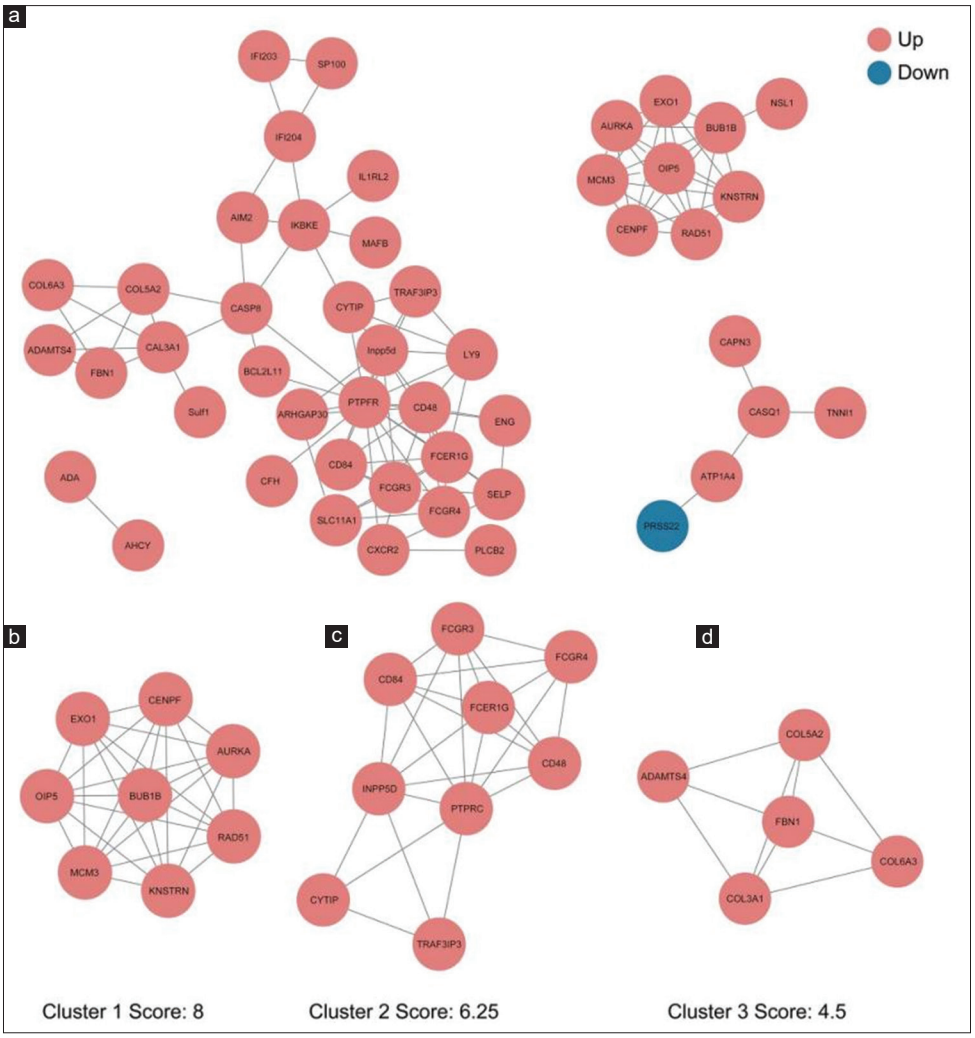

Figure 3: Protein–protein interaction network and cluster modules of the differentially expressed genes (DEGs). (a) The interaction network between proteins coded by the DEGs. Each node represents a protein, while each edge represents one protein–protein association. Three cluster modules were extracted by Minimal Common Oncology Data Elements (b-d). Up represents upregulated genes, down represents downregulated genes in test datasets GSE74052 and GSE137482

CENPF (AUC: 0.667), CD84 (AUC: 0.667), AURKA (AUC: 0.633), RAD51 (AUC: 0.600), and KNSTRN (AUC: 0.567) [Figure 5].

Validation of hub genes by GSE131193

GEO dataset GSE131193 containing 3 IS brain microvessel samples and 3 control was also used to validate the 8 hub genes. It was found that the expression of AURKA, CENPF, CD84, KNSTRN, and MCM3 was markedly upregulated in IS group when compared with control; however, OIP5, EXO1, and RAD51 showed no significant differences [Figure 6].

Verification of key genes by quantitative reverse transcription-polymerase chain reaction

Above validation tests suggested that five hub genes (AURKA, CENPF, CD84, KNSTRN, and MCM3) might be key gene candidates during IS pathogenesis. We then further verified them five by qRT-PCR experiments using bEnd. 3 cell cultures with OGD challenge. It was found that the expression of CENPF and AURKA increased significantly at 12 h or 24 h after OGD insult when compared with normoxia control [Figure 7a and b]. Therefore, we hypothesized that the two genes AURKA and CENPF might serve as target genes for treating IS.

Construction of competitive endogenous RNA network

Recently, miRNAs have been found to act as an important part in posttranscriptional regulation of gene expression and RNA silencing in brain health and disease.[28-30] Their upstream molecules, lncRNAs and circRNAs, can combine miRNA response elements to affect the function of miRNAs, thus upregulating gene expression. This RNAs interaction is called a ceRNA network.[31] Using our former dataset containing 118 significantly expressed miRNAs in IS mouse brains[25] as well as online NetworkAnalyst,[32] we obtained 6 significantly expressed miRNAs targeting

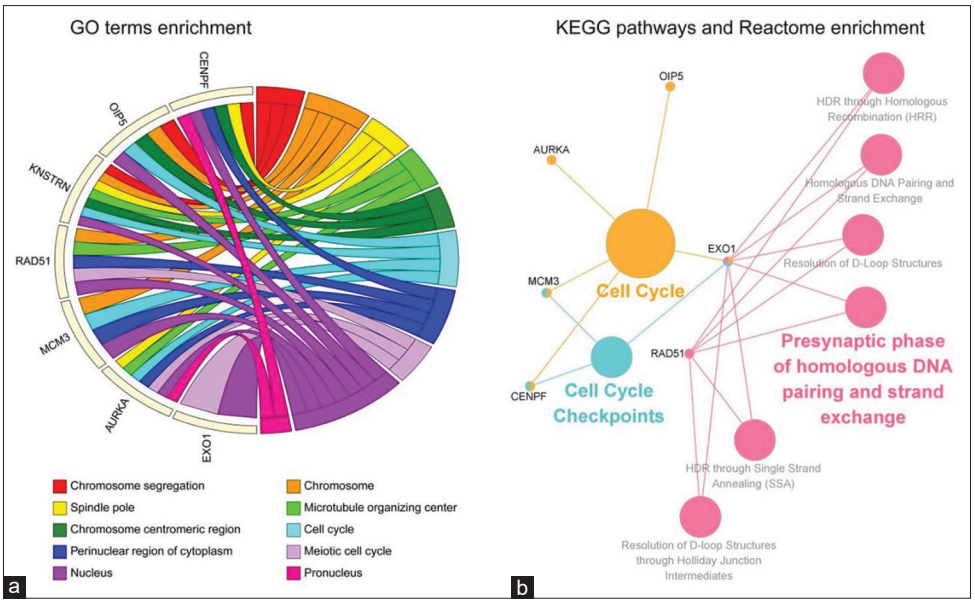

Figure 4: Functional enrichment analysis of the 8 hub genes. (a) The chord plot showed the top 10 enriched Gene Ontology terms of the hub genes. (b) The network of significant Kyoto Encyclopedia of Genes and Genomes and reactome enriched pathways of the hub genes based on their functions. Color circles represent categories of pathway terms; The larger the circle diameter, the larger the significance. GO: Gene ontology, KEGG: Kyoto encyclopedia of genes and genomes, SSA: Single strand annealing, HRR: Homologous recombination repair, HDR: Homology dependent repair

genes AURKA and CENPF. They were AUKRA-related miR-666-3p and CENPF-associated miR-384-5p/miR-34b-3p/miR-770-5p/miR-337-3p/miR-297b-3p. After then, the six selected miRNAs-interacted circRNAs and lncRNAs were predicted through the online database Starbase. The screening criteria to predict lncRNAs were mammalian, mouse genome, and low stringency (≥1) of CLIP-Data. The screening criteria to predict circRNAs were mammalian, mouse genome, medium stringency (≥2) of CLIP-Data. The 12 target lncRNAs and 6 target circRNAs of AURKA-targeted miR-666-3p were obtained. The 31 target lncRNA and 34 target circRNAs of the 5 target miRNAs of CENPF were obtained. The ceRNA network was created and illustrated by Cytoscape [Figure 7c]. According to the ceRNA results, we ultimately selected two downregulated miRNAs (miR-34b-3p and miR-297b-3p) and their four upregulated lncRNAs (Malat1, Xist, Snhg12, Mir17 hg) in IS. The prediction results of ceRNAs proposed that the RNA pathways Malat1/Snhg12/Xist-miR-297b-3p-CENPF as well as Mir17 hg-miR-34b-3p-CENPF could be potential therapeutic targets for IS.

Discussion

Limited treatment options of IS call for better understanding of pathological process of IS and identifying effective molecular/cellular targets for therapeutic strategy. Currently, BBB and microvasculature impairment stands as a key pathological manifestation of IS,[33,34] which has greatly highlighted the feasibility to investigate new approaches to target pro-inflammatory EC events to arrest pathogenic process of IS.

In this study, 84 ischemic brain EC-specific DEGs were identified. GO, KEGG, and reactome enrichment analysis all characterized the ischemic cerebral ECs with strong immune activation. GO enrichment analysis and reactome reaction analysis indicated that the DEGs were mainly enriched in immune responses such as T cell activation and immune system processes, cell–surface interactions on vascular wall, and degradation of extracellular matrix. KEGG pathways of the DEGs consisted of tuberculosis, protein digestion and absorption, NOD-like receptor signaling pathway, lipid and atherosclerosis, *S. aureus* infection, and thyroid hormone synthesis. After screening DEGs through PPI network, we obtained 8 ischemic EC-specific hub genes in IS. Then, we further validated the hub genes by other GEO datasets. Validation tests recommended 5 hub genes with significantly enhanced expression in ischemic brain microvessel ECs, including AURKA, CENPR, CD84, KNSTRN, and MCM3. Next, using EC cultures with *in vitro* ischemic condition, we performed RT-PCR test to further identify the key genes. Finally, we hypothesized that AURKA and CENPF may serve as brain EC-specific key genes of interest for IS therapy.

AURKA is originally recognized as an overexpressed serine/threonine kinase in cancers, and its activation is essential for the process of cell division by regulating mitosis.[35] AURKA is a critical upstream regulator of HIF1 transcription complex,[36] and its expression is common

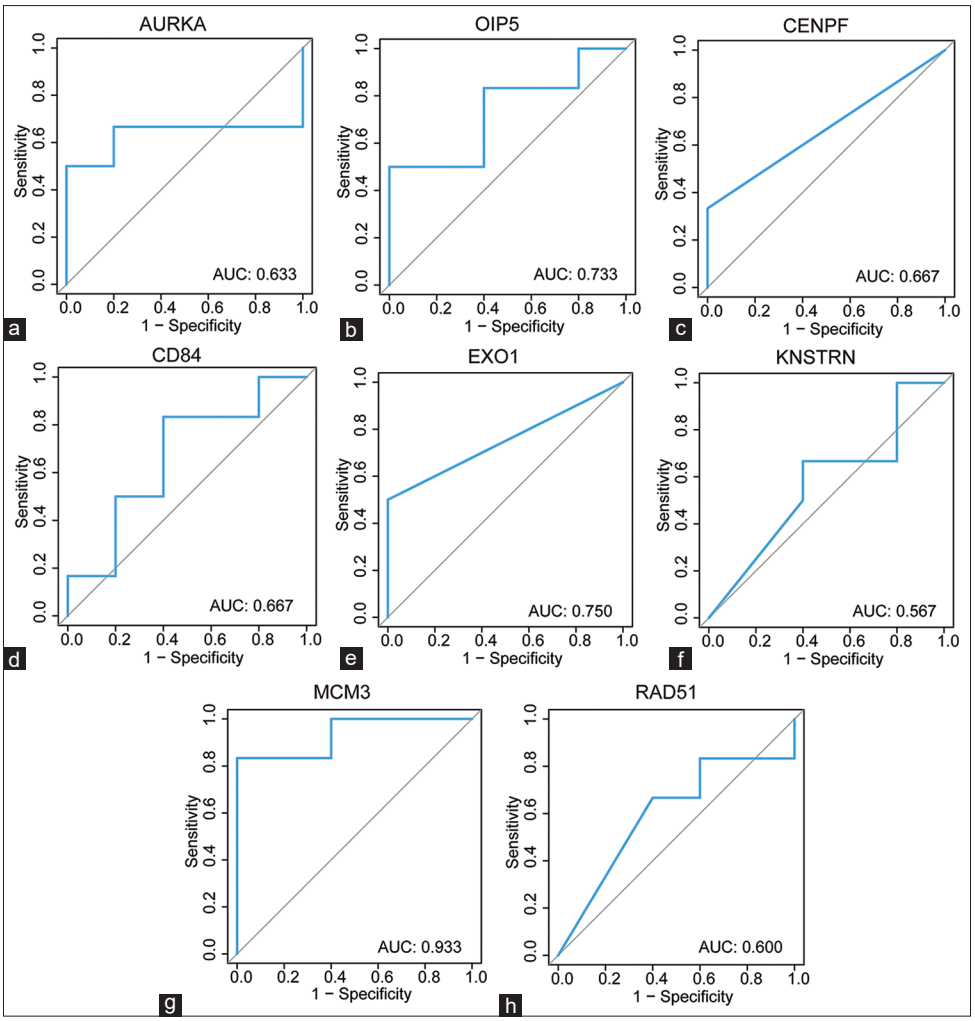

Figure 5: Receiver operating characteristic (ROC) curve of the 8 hub genes by GSE163752. (a-h) ROC curve of AURKA, OIP5, CENPF, CD84, EXO1, KNSTRN, MCM3, and RAD51 in established ischemic endothelial cells samples. AUC: Area under the ROC curve, ROC: Receiver operating characteristic

under metabolic stress including hypoxia and glucose starvation.[37] Beside nucleus, AURKA is located in the mitochondria, which can affect organelle dynamics and regulate energy production.[38,39] Numerous studies have reported that AURKA is essential for angiogenesis by impacting EC polarization and directional migration.[40,41] In this study, the mRNA level of AURKA was found significantly elevated at 24 h in bEnd. 3 cells with 1 h-OGD challenge, indicating its involvement in the pathogenesis of brain ECs in IS.

The other selected key gene, CENPF, is a mitotic cell cycle-associated gene which encodes a mitotic centromere protein.[42] The aberrantly upregulated expression of CENPF was recorded in several cancers.[43-45] CENPF depletion caused proliferation defect, cell cycle arrest, and apoptosis in thyroid cancer cells,[46] while CENPF overexpression inhibited cell apoptosis and promoted cell proliferation under endoplasmic reticulum stress in human osteosarcoma cells.[47] Here, our laboratory study detected that the mRNA level of CENPF increased obviously in bEnd. 3 cells at 12 h after OGD treatment. The data demonstrated that CENPF might be a novel candidate gene of interest to take action in ischemia-induced stress response of brain ECs in IS.

In addition, target miRNAs, lncRNAs, and circRNAs for AURKA and CENPF were predicted, and a ceRNA network with Cytoscape was developed. Among the target miRNAs, the levels of miR-297b-3p and miR-34b-3p were downregulated; on the contrary, miR-337-3p, miR-384-5p, miR-770-5p, and miR-666-3p were upregulated in early IS.[25] Due to our previous data plus ceRNA hypothesis, we proposed that the following lncRNA-miRNA-mRNA pathways: Malat1/Snhg12/Xist-miR-297b-3p-CENPF, Mir17hg-miR-34b-3p-CENPF, were potential RNA regulatory pathways against the pathogenesis of early IS. Moreover, we conducted a literature research and confirmed the functional involvement of above-mentioned upregulated lncRNAs in IS.[48-50] Specially, lncRNA Malat1 was currently a hot research topic for its anti-apoptotic and

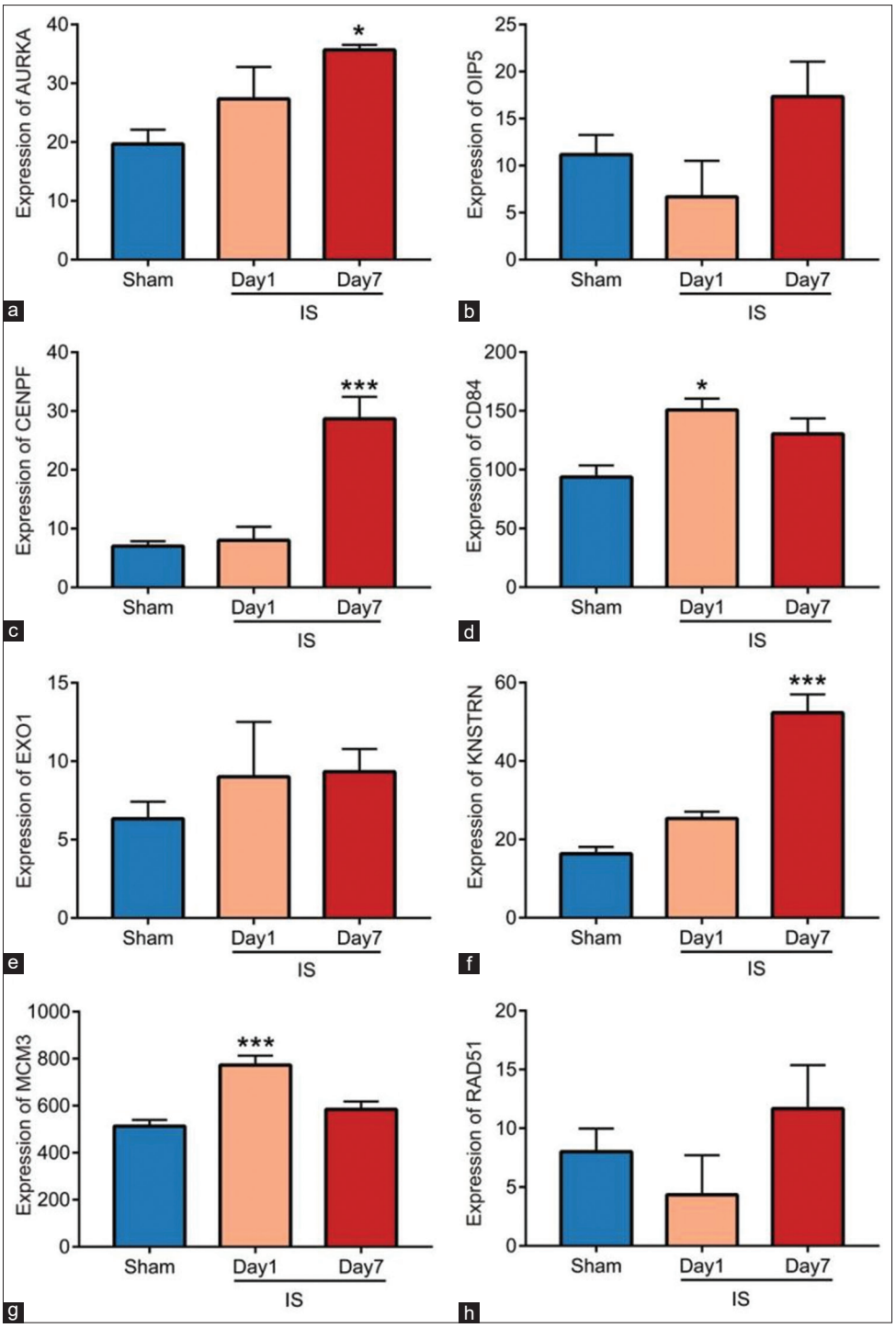

Figure 6: Validation of the hub genes by GSE131193. (a-h) The expressions of AURKA, OIP5, CENPF, CD84, EXO1, KNSTRN, MCM3 and RAD51 in mouse brain microvessles of ischemic stroke compared with control. *P < 0.05, ***P < 0.001. IS: Ischemic stroke

anti-inflammatory effects in cerebrovasculature to reduce brain ischemic damages.[48,51]

Conclusions

We identified two brain vascular EC-specific expressed genes, AURKA and CENPF, as potential therapeutic targets of IS at the transcriptome level using integrated bioinformatical analysis. Furthermore, regarding the ceRNA results, we proposed that the lncRNAs Malat1, Snhg12, and Xist that targeted miR297b-3p-CENPF axis, as well as Mir17 hg which targeted miR34b-3p-CENPF, might be potential RNA-regulatory pathways to regulate BBB function in IS. However, one limitation of this study is the relatively small sample size for analysis and validation. Accordingly, it is necessary for future studies

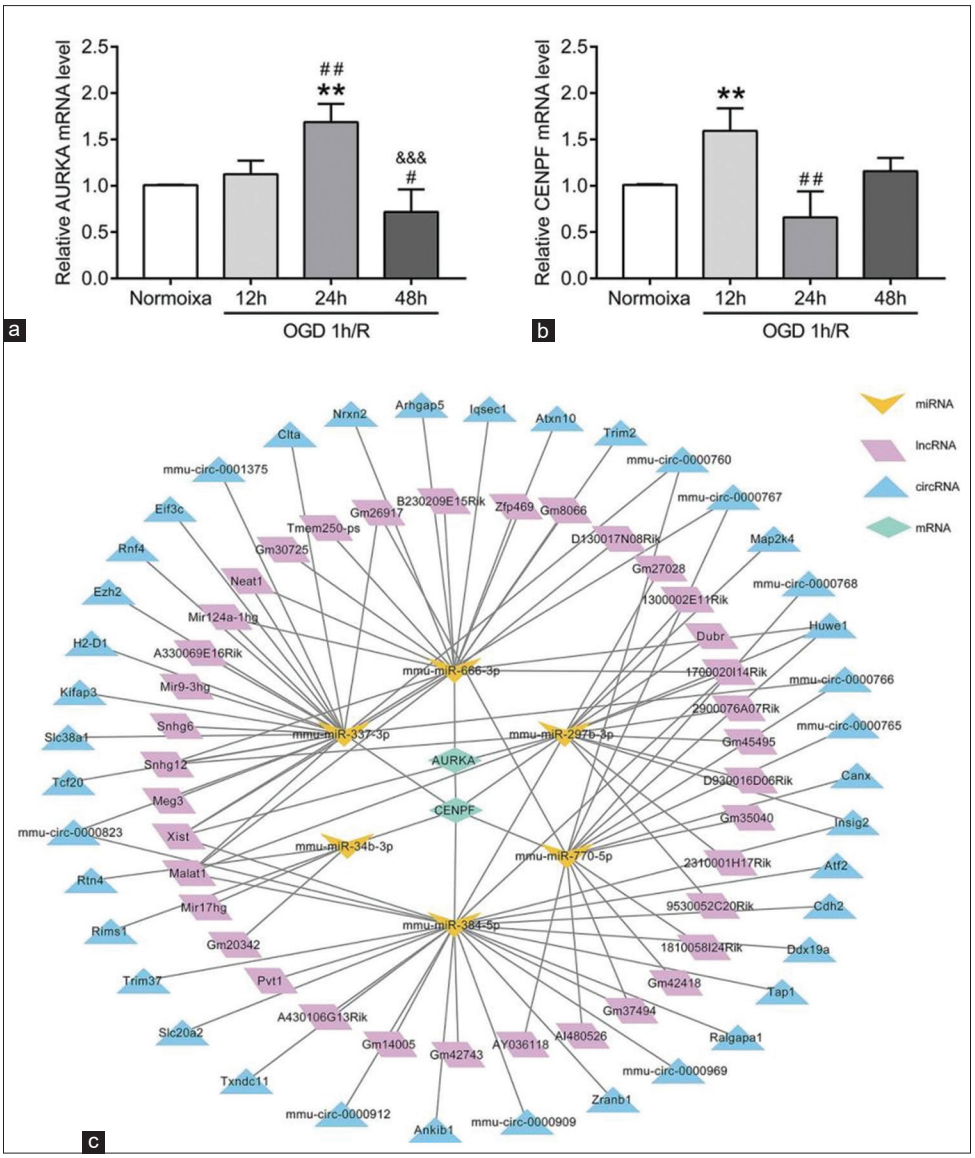

Figure 7: Reverse transcription-polymerase chain reaction verification of AURKA and CENPF and their competitive endogenous RNA (ceRNA) network. (a) Relative expression of AURKA. (b) Relative expression of CENPF; n = 5–6; $^{**}P < 0.01$, compared with normoxia. $^{\#}P < 0.05$, $^{\#\#}P < 0.01$ compared with oxygen-glucose deprivation (OGD) 1 h/R 12 h; $^{\&\&\&}P < 0.001$, compared with the OGD 1 h/R 24 h. (c) Co-expressed ceRNA network of AURKA and CENPF. The green diamonds represent the hub genes, the yellow V represents microRNA, purple parallelograms represent lncRNAs, and blue triangles represent circRNAs. OGD: Oxygen-glucose deprivation

to expand the sample size and conduct experiments to confirm the results.

Ethical statement

Not applicable.

Data availability statement

The datasets generated during and/or analyzed during the current study are available from the corresponding author on reasonable request.

Author contributions

YZ and LZ conceived and designed the experiments; YY, YZ, and LZ performed the experiments and analyzed the data; YY, YZ, and LZ wrote and revised the manuscript; and ZW, XL, SH, and JL offered technical support.

Financial support and sponsorship

This work was supported by the Beijing Natural Science Foundation (7232003, 7232006) and the National Natural Science Foundation of China (82071539).

Conflicts of interest

There are no conflicts of interest.

References

1. Campbell BC, De Silva DA, Macleod MR, Coutts SB, Schwamm LH,

Davis SM, *et al*. Ischaemic stroke. Nat Rev Dis Primers 2019;5:70.
2. Kurian C, Mayer S, Kaur G, Sahni R, Feldstein E, Samaan M, *et al.* Bihemispheric ischemic strokes in patients with COVID-19. Brain Circ 2022;8:10-6.
3. Xiong Y, Wakhloo AK, Fisher M. Advances in acute ischemic stroke therapy. Circ Res 2022;130:1230-51.
4. Sandset EC, Goldstein LB. Advances in stroke: Treatments-preventive. Stroke 2022;53:608-10.
5. Li G, Liu P, Gong W, Zhang X, Zhang Y, Wang N. Endovascular recanalization for symptomatic intracranial internal carotid and middle cerebral artery occlusion lasting longer than 72 h: Experience in a single center. Brain Circ 2021;7:259-64.
6. Taylor BE, Patel S, Hilden P, Otite FO, Lee K, Gupta G, *et al.* The weekend effect on mechanical thrombectomy: A nationwide analysis before and after the pivotal 2015 trials. Brain Circ 2022;8:137-45.
7. Amado B, Melo L, Pinto R, Lobo A, Barros P, Gomes JR. Ischemic stroke, lessons from the past towards effective preclinical models. Biomedicines 2022;10:2561.
8. Yang C, Hawkins KE, Doré S, Candelario-Jalil E. Neuroinflammatory mechanisms of blood-brain barrier damage in ischemic stroke. Am J Physiol Cell Physiol 2019;316:C135-53.
9. Shekhar S, Cunningham MW, Pabbidi MR, Wang S, Booz GW, Fan F. Targeting vascular inflammation in ischemic stroke: Recent developments on novel immunomodulatory approaches. Eur J Pharmacol 2018;833:531-44.
10. Tuo QZ, Zhang ST, Lei P. Mechanisms of neuronal cell death in ischemic stroke and their therapeutic implications. Med Res Rev 2022;42:259-305.
11. Saft M, Gonzales-Portillo B, Park YJ, Cozene B, Sadanandan N, Cho J, *et al.* Stem cell repair of the microvascular damage in stroke. Cells 2020;9:2075.
12. Abdullahi W, Tripathi D, Ronaldson PT. Blood-brain barrier dysfunction in ischemic stroke: Targeting tight junctions and transporters for vascular protection. Am J Physiol Cell Physiol 2018;315:C343-56.
13. Vogelstein B, Papadopoulos N, Velculescu VE, Zhou S, Diaz LA Jr., Kinzler KW. Cancer genome landscapes. Science 2013;339:1546-58.
14. Li X, Wang CY. From bulk, single-cell to spatial RNA sequencing. Int J Oral Sci 2021;13:36.
15. Shen L, Zhou K, Liu H, Yang J, Huang S, Yu F, *et al.* Prediction of mechanosensitive genes in vascular endothelial cells under high wall shear stress. Front Genet 2021;12:796812.
16. Zhu B, Liu W, Xu Q, Liu HL. MicroRNA-486-5p functions as a diagnostic marker for carotid artery stenosis and prevents endothelial dysfunction through inhibiting inflammation and oxidative stress. Bioengineered 2022;13:8667-75.
17. Zhao B, Jiang X. hsa-miR-518-5p/hsa-miR-3135b regulates the REL/SOD2 pathway in ischemic cerebral infarction. Front Neurol 2022;13:852013.
18. Cheng Q, Chen X, Wu H, Du Y. Three hematologic/immune system-specific expressed genes are considered as the potential biomarkers for the diagnosis of early rheumatoid arthritis through bioinformatics analysis. J Transl Med 2021;19:18.
19. Guo Y, Bao Y, Ma M, Yang W. Identification of key candidate genes and pathways in colorectal cancer by integrated bioinformatical analysis. Int J Mol Sci 2017;18:722.
20. Wang H, Zhu H, Zhu W, Xu Y, Wang N, Han B, *et al.* Bioinformatic analysis identifies potential key genes in the pathogenesis of turner syndrome. Front Endocrinol (Lausanne) 2020;11:104.
21. Luan H, Zhang C, Zhang T, He Y, Su Y, Zhou L. Identification of key prognostic biomarker and its correlation with immune infiltrates in pancreatic ductal adenocarcinoma. Dis Markers 2020;2020:8825997.
22. Yang X, Li Y, Lv R, Qian H, Chen X, Yang CF. Study on the multitarget mechanism and key active ingredients of Herba Siegesbeckiae and volatile oil against rheumatoid arthritis based on network pharmacology. Evid Based Complement Alternat Med 2019;2019:8957245.
23. Ge X, Tang P, Rong Y, Jiang D, Lu X, Ji C, *et al.* Exosomal miR-155 from M1-polarized macrophages promotes EndoMT and impairs mitochondrial function via activating NF-κB signaling pathway in vascular endothelial cells after traumatic spinal cord injury. Redox Biol 2021;41:101932.
24. Liu Y, Yuan Y, Yan Y, Wang R, Wang Z, Liu X, *et al.* Mitochondrial pyruvate carrier 1 alleviates hypoxic-ischemic brain injury in rats. Life Sci 2023;325:121686.
25. Liu C, Zhao L, Han S, Li J, Li D. Identification and functional analysis of microRNAs in mice following focal cerebral ischemia injury. Int J Mol Sci 2015;16:24302-18.
26. Li JH, Liu S, Zhou H, Qu LH, Yang JH. starBase v2.0: Decoding miRNA-ceRNA, miRNA-ncRNA and protein-RNA interaction networks from large-scale CLIP-Seq data. Nucleic Acids Res 2014;42:D92-7.
27. de Hond AA, Steyerberg EW, van Calster B. Interpreting area under the receiver operating characteristic curve. Lancet Digit Health 2022;4:e853-5.
28. Yang K, Zeng L, Ge A, Wang S, Zeng J, Yuan X, *et al*. A systematic review of the research progress of non-coding RNA in neuroinflammation and immune regulation in cerebral infarction/ischemia-reperfusion injury. Front Immunol 2022;13:930171.
29. Yuan L, Chen W, Xiang J, Deng Q, Hu Y, Li J. Advances of circRNA-miRNA-mRNA regulatory network in cerebral ischemia/reperfusion injury. Exp Cell Res 2022;419:113302.
30. Mehta SL, Chokkalla AK, Vemuganti R. Noncoding RNA crosstalk in brain health and diseases. Neurochem Int 2021;149:105139.
31. Salmena L, Poliseno L, Tay Y, Kats L, Pandolfi PP. A ceRNA hypothesis: The Rosetta Stone of a hidden RNA language? Cell 2011;146:353-8.
32. Pound P, Ram R. Are researchers moving away from animal models as a result of poor clinical translation in the field of stroke? An analysis of opinion papers. BMJ Open Sci 2020;4:e100041.
33. Li W, Pan R, Qi Z, Liu KJ. Current progress in searching for clinically useful biomarkers of blood-brain barrier damage following cerebral ischemia. Brain Circ 2018;4:145-52.
34. Ozaki T, Nakamura H, Kishima H. Therapeutic strategy against ischemic stroke with the concept of neurovascular unit. Neurochem Int 2019;126:246-51.
35. Du R, Huang C, Liu K, Li X, Dong Z. Targeting AURKA in cancer: Molecular mechanisms and opportunities for cancer therapy. Mol Cancer 2021;20:15.
36. Whately KM, Voronkova MA, Maskey A, Gandhi J, Loskutov J, Choi H, *et al.* Nuclear aurora-A kinase-induced hypoxia signaling drives early dissemination and metastasis in breast cancer: Implications for detection of metastatic tumors. Oncogene 2021;40:5651-64.
37. Hamidi T, Cano CE, Grasso D, Garcia MN, Sandi MJ, Calvo EL, *et al.* Nupr1-aurora kinase A pathway provides protection against metabolic stress-mediated autophagic-associated cell death. Clin Cancer Res 2012;18:5234-46.
38. Bertolin G, Bulteau AL, Alves-Guerra MC, Burel A, Lavault MT, Gavard O, *et al.* Aurora kinase A localises to mitochondria to control organelle dynamics and energy production. Elife 2018;7:e38111.
39. Bertolin G, Tramier M. Insights into the non-mitotic functions of aurora kinase A: More than just cell division. Cell Mol Life Sci 2020;77:1031-47.
40. Ki SM, Kim JH, Won SY, Oh SJ, Lee IY, Bae YK, *et al.* CEP41-mediated ciliary tubulin glutamylation drives angiogenesis through AURKA-dependent deciliation. EMBO Rep 2020;21:e48290.
41. Xu Y, Wang C, Chen X, Li Y, Bian W, Yao C. San Huang decoction targets aurora kinase a to inhibit tumor angiogenesis in breast cancer. Integr Cancer Ther 2020;19:1534735420983463.

42. Shahid M, Lee MY, Piplani H, Andres AM, Zhou B, Yeon A, *et al.* Centromere protein F (CENPF), a microtubule binding protein, modulates cancer metabolism by regulating pyruvate kinase M2 phosphorylation signaling. Cell Cycle 2018;17:2802-18.
43. Huang YG, Li D, Wang L, Su XM, Tang XB. CENPF/CDK1 signaling pathway enhances the progression of adrenocortical carcinoma by regulating the G2/M-phase cell cycle. J Transl Med 2022;20:78.
44. Chen EB, Qin X, Peng K, Li Q, Tang C, Wei YC, *et al.* HnRNPR-CCNB1/CENPF axis contributes to gastric cancer proliferation and metastasis. Aging (Albany NY) 2019;11:7473-91.
45. Zou PA, Yang ZX, Wang X, Tao ZW. Upregulation of CENPF is linked to aggressive features of osteosarcoma. Oncol Lett 2021;22:648.
46. Han Y, Xu S, Cheng K, Diao C, Liu S, Zou W, *et al.* CENPF promotes papillary thyroid cancer progression by mediating cell proliferation and apoptosis. Exp Ther Med 2021;21:401.
47. Shen T, Li Y, Liang S, Chen Z. XBP1 negatively regulates CENPF expression via recruiting ATF6α to the promoter during ER stress. Cancer Cell Int 2020;20:459.
48. Cao Y, Liu J, Lu Q, Huang K, Yang B, Reilly J, *et al.* An update on the functional roles of long non-coding RNAs in ischemic injury (review). Int J Mol Med 2022;50:91.
49. Huang H, Wei G, Wang C, Lu Y, Liu C, Wang R, *et al*. A functional polymorphism in the promoter of miR-17-92 cluster is associated with decreased risk of ischemic stroke. BMC Med Genomics 2019;12:159.
50. Xiao FJ, Zhang D, Wu Y, Jia QH, Zhang L, Li YX, *et al.* miRNA-17-92 protects endothelial cells from erastin-induced ferroptosis through targeting the A20-ACSL4 axis. Biochem Biophys Res Commun 2019;515:448-54.
51. Zhang X, Tang X, Liu K, Hamblin MH, Yin KJ. Long noncoding RNA malat1 regulates cerebrovascular pathologies in ischemic stroke. J Neurosci 2017;37:1797-806.